Physics-based Modeling of Skier Mobility and Avalanche Rescue in Mountainous Terrain

Xin Liu, Carey Williamson, and Jon Rokne
Department of Computer Science
University of Calgary
Calgary, Alberta, Canada
Email: {liuxin,carey,rokne}@cpsc.ucalgary.ca

***Abstract*—Mobility models play an important role in the evaluation of wireless ad hoc networks. However, most existing mobility models are limited to 1D or 2D user movement. In this paper, we propose a novel 2.5D mobility model suitable for modeling the movement of backcountry skiers in mountainous terrains. These skiers carry wireless devices for communication in the event of emergencies, such as an avalanche, and thus form a dynamic mobile wireless ad hoc network. Our model represents groups of skiers, with each group having an invisible leader who determines the general direction of movement. We calculate the acceleration, velocity, and position of the group leader based on properties of the terrain, gravitational force, and a randomized sine function. To simulate the coordinated mobility of group members, we use a flocking model, which applies cohesion, separation, and alignment forces to influence group members to follow their leader, while avoiding collisions with each other. To demonstrate the applicability of our model, we use simulation to evaluate the skier rescue probability in the event of an avalanche.**

Keywords: Mobility model, Flocking model, Skier mobility, Avalanche safety, Wireless ad hoc networks, Simulation

I. Introduction

Mobility models are used to represent the movement of mobile users, and how their locations, directions, and velocities change over time. Such models are frequently used in simulation studies to investigate the performance of communication protocols in wireless ad hoc networks. In many cases, the simulation results obtained are highly sensitive to the specific mobility model used [1]. Therefore, building realistic mobility models is a key issue in the simulation-based performance evaluation of wireless ad hoc networks.

In this paper, we study the problem of mobility modeling for backcountry skiers in mountainous terrains. These skiers eschew the carefully groomed slopes and massive crowds of popular ski resorts, preferring instead the adrenaline rush of rugged outdoor adventure in remote and relatively unexplored terrain. While there are risks associated with this activity (e.g., getting lost or injured, or caught in an avalanche), most such skiers are responsible and well-prepared. In particular, they carry wireless devices, such as cell phones, avalanche beacons, or wireless transponders as safety measures for emergency situations. Furthermore, they usually travel in groups.

Our work is motivated by the following research question: in the event of an avalanche, what is the probability of being rescued if you are buried? We are also interested in the effects of mobility pattern, group size, wireless communication range, skiing velocity, and avalanche magnitude on the rescue probability. We explore these issues by building a detailed skier mobility model, and simulating avalanche events.

Our paper makes two main contributions. First, we develop a physics-based model of skier mobility in mountainous regions. We refer to our model as a 2.5D model, since it has movement in the x, y, and (limited) z dimensions. The proposed *skiing mobility model* considers the physical effects of gravity and the steepness of the terrain. We also use a flocking model to simulate the movement of groups of skiers. Second, we use our model to evaluate the effectiveness of wireless communication devices in improving avalanche safety. Specifically, we use simulation to evaluate the rescue probabilities for backcountry skiers caught in the path of an avalanche.

The rest of this paper is organized as follows. Section II reviews prior related work on user mobility modeling in wireless ad hoc networks. Section III introduces our proposed skier mobility model, while Section IV presents the details of the model. Section V presents simulation results obtained using our model. Finally, Section VI concludes the paper.

II. Related Work

There are many papers on mobility modeling. In this section, we briefly review those most relevant to our work, particularly for low-rate (pedestrian) and high-rate (vehicular) movement. Interested readers may refer to survey papers [1], [2] for a fuller treatment of mobility modeling techniques.

Most mobility models work in *two-dimensional* (2D) planar regions. The *random walk mobility model* [1], [3], [4], also called *Brownian motion*, is a simple 2D model that is widely used by networking researchers. In this model, a Mobile Node (MN) moves from its current location to a new location with randomly selected direction and speed. The MN arrives at its new location after a constant time interval or a constant distance. It then selects a new direction and speed and heads to the next location. The Brownian motion is *memoryless*, because the MN's speed and direction are independent of their previous values. This will produce zigzag trajectories that differ from real-world (human) movements.

A reasonably smooth motion path can be produced by the *boundless simulation area mobility model* [1], [5]. In this more advanced model, the current direction $\theta(t)$ and speed $v(t)$ of travel is related to the previous direction and speed and is updated at discrete times Δt. This allows the MN to proceed smoothly along curves.

The *random waypoint mobility model* is a variant of the random walk mobility model that is widely used in ad hoc network performance evaluations [1], [4], [6], [7]. The new feature in the random waypoint mobility model is a *pause time* that occurs between changes in direction and/or speed. When applied to ad hoc networks, the simulation results for the random waypoint mobility model are highly dependent on the MN's speed and pause time.

Hsu *et al.* proposed a *weighted waypoint mobility model* [8] to characterize pedestrian mobility patterns to and from preferred locations in a campus environment. This is done by defining popular locations in the simulation area and assigning different "weights" to them according to the probability of choosing that destination.

The *Gauss-Markov mobility model* [1], [9] was designed to represent different levels of randomness in time and space. Initially, each MN is assigned a speed and direction. The Gauss-Markov mobility model then updates the speed s_n and direction d_n of each MN at fixed time intervals based on their previous values s_{n-1}, d_{n-1} and two Gaussian distributed random variables. A *tuning parameter* α $(0 \leq \alpha \leq 1)$ is used to vary the randomness.

In the aforementioned mobility models, the MNs move independently. However, in real-world scenarios, groups of MNs often move together. For example, soldiers in a battlefield usually move in groups to accomplish certain tasks. This requires a *group mobility model*. There are many papers on this topic [1], [10], [11], [12]. The *exponential correlated random mobility model* [13] generates movement for both individuals and groups, by adjusting the parameters of a motion function. The new position $\vec{b}(t+1)$ at time $t+1$ is a function of the previous position $\vec{b}(t)$ at time t and a Gaussian random variable, with parameters potentially varying from group to group. The drawback of this model is that it is not easy to enforce a given motion pattern by selecting the parameters.

The *reference point group mobility model* [12] is a more flexible group model. In this model (see Fig. 1), each group has a "center" that determines the entire group's motion behavior, including acceleration, speed, direction, and location. The motion of each group is explicitly defined by a *motion path*. A motion path is given by defining a sequence of *check points* along the path corresponding to given time intervals. Nodes are uniformly distributed within the geographic scope of a group. Each node is assigned a *reference point* that follows the group's movement. A node is randomly placed in the neighborhood of its reference point at each step. The reference point scheme allows independent random motion behavior for each node, in addition to the group motion.

The *reference region group mobility model* [10], [11] is a group model that can produce group partitioning and merging.

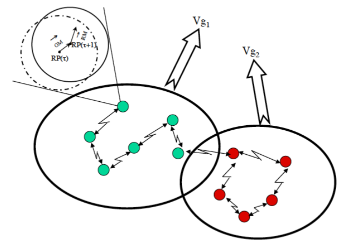

Fig. 1. The reference point group mobility model [12].

In this model, every group is associated with a *reference region* that is an area that nodes will move towards. When a group arrives at the reference region, the nodes will move around within the region waiting for the arrival of others. After a reference region has been stationary for some time at an intermediate location, a new location for the reference region will be generated. Then the reference region moves gradually towards the destination with its path defining the trajectory of the movement of the group. New destinations may be created so that if multiple destinations are assigned to a group, this group will be partitioned into some smaller subgroups, each with a new reference region associated to a different destination. When a group reaches its destination, the group can merge with another group.

Higher-velocity movement patterns have been studied in Vehicular Ad-hoc Networks (VANETs), where the mobility of vehicles are studied [14]. Because vehicles tend to follow roads, these models usually constrain the mobility to line segments embedded in a 2D plane. A good example is the *freeway mobility model* [15] for simulating the movement of mobile nodes (MNs) on a highway. In this model, each mobile node is restricted to its lane on the freeway. The velocity of an MN is temporally dependent on its previous velocity. If two MNs on the same freeway lane are within some safety distance, the velocity of the following MN cannot exceed the velocity of preceding MN. An extension of this model, called the Manhattan model, simulates the movement pattern of MNs on a grid of city streets defined by maps.

III. Skier Mobility Model

A. Model Overview

Our *skiing mobility model* is built in a 2.5D terrain space. Here 2.5D means that each point on the terrain surface is completely described by a 2D coordinate on the horizontal plane plus a height value. (Since each 2D coordinate can only have one height value, such models are not truly 3D.) The mobility model consists of *skier groups*. We assign an *invisible leader* to each skier group. The invisible leader is not a member of the group, but determines the overall movement of the group. The leader advances along a random S-shaped trajectory, swaying left and right around the *fastest descent direction* (also known as the "fall line") on the terrain surface. The instantaneous acceleration is constrained by the gravitational acceleration modified by the inclination angle of advance. The speed varies within a user-designated scope.

Each group is composed of one or more skiers. The movement of each skier is determined by a *flocking model* [16], which attracts skiers towards the invisible leader, avoids collisions, and coordinates the actions of group members based on three virtual forces.

Our mobility model of the invisible leader is similar to the *boundless simulation area mobility model* [5]. However, we compute the advance direction based on a randomized sine function, and compute the acceleration based on the advance direction, the terrain's steepness, and the gravitational acceleration. This makes our mobility model highly realistic.

Our group mobility model is similar to the *reference point group mobility model* [12]. However, we calculate the invisible leader's movement automatically and employ the *flocking model*, which organizes the skier group with virtual forces. This provides greater flexibility and produces more life-like motion patterns than the reference point based method [12].

The proposed skiing mobility model can be used for evaluating wireless ad hoc protocols. In this paper, we present an example of using our skier mobility model to evaluate avalanche rescue probabilities for backcountry skiers equipped with wireless devices.

B. Model Preliminaries and Notation

In this section, we review the basic geometric and physical properties of our system model, and define our model notation.

A *terrain* $\mathcal{S}$ is defined as a single-valued differentiable function on a 2D space, where $z = h(x, y)$. As shown in Fig. 2, a point P on $\mathcal{S}$ has 3D coordinates (x_P, y_P, z_P).

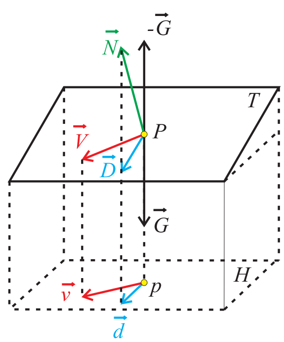

Fig. 2. Vectors related to a point P on the terrain.

There are some important geometric elements for modeling the mobility of skiers related to the point P and terrain $\mathcal{S}$:

- H: the horizontal plane

  H is physically horizontal. It is also the 2D (x, y) parametric space.
- p: the vertical projection of P on H

  p has a 2D coordinate (x_P, y_P).
- $\vec{G}$: the gravity vector

  $\vec{G}$ is perpendicular to H. $\left|\vec{G}\right| \approx 9.81$ m/s^2 is called the *gravitational constant*.
- $-\vec{G}$: the opposing (negative) gravity vector
- T: the tangential plane

  The tangential plane is defined by

$$h'_x(x_P, y_P) \cdot (x - x_P) + h'_y(x_P, y_P) \cdot (y - y_P) - (z - z_P) = 0. \quad (1)$$

- $\vec{N}$: the normal vector of the surface

  $\vec{N}$ is perpendicular to T, which is defined by

$$\vec{N} = \left(-h'_x(x_P, y_P), -h'_y(x_P, y_P), 1\right). \quad (2)$$

- $\vec{d}$: the negative gradient vector

  $\vec{d}$ is the vertical projection of $\vec{N}$ on the 2D horizontal plane, denoting the fastest descent direction of z in the (x, y) parametric space. It is defined by

$$\vec{d} = \left(-h'_x(x_P, y_P), -h'_y(x_P, y_P)\right). \quad (3)$$

- $\vec{D}$: the fastest descent vector on $\mathcal{S}$

  $\vec{D}$ is the vertical projection of $\vec{d}$ on the tangential plane T.
- $\vec{V}$: the skier's velocity

  $\vec{V}$ is a 3D vector on the tangential plane. $\left|\vec{V}\right|$ is a scalar called the skier's speed.
- $\vec{v}$: the 2D velocity on H

  $\vec{v}$ is the 2D vertical projection of $\vec{V}$ on H. It denotes the direction and speed that a skier is moving in the (x, y) parametric space.
- ϕ: the inclination angle of the terrain at P

$$\phi = \angle\widehat{\vec{N}\left(-\vec{G}\right)}. \quad (4)$$

- θ: the azimuth angle of advance

$$\theta = \angle\widehat{\vec{v}\vec{d}}. \quad (5)$$

- φ: the inclination angle of advance

$$\varphi = \angle\widehat{\vec{V}\vec{G}}. \quad (6)$$

As shown in Fig. 3, the inclination angle of advance can be computed by trigonometry:

$$\cos\varphi = \frac{\tan\phi}{\sqrt{\tan^2\phi + \cos^{-2}\theta}}. \quad (7)$$

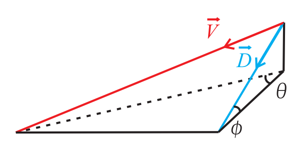

Fig. 3. Computing the inclination angle of advance.

C. Terrain Model

We consider two mathematical terrain models, which are the *cone model* and the *Gaussian model* (see Fig. 4).

1) Simple Conic Model: Fig. 4(a) shows a conic model with base radius $\tilde{r}$ and height $\tilde{h}$. Its surface is given by:

$$z = \begin{cases} \tilde{h} - \frac{\tilde{h}}{\tilde{r}}\sqrt{x^2+y^2}, & \text{if } x^2+y^2 < \tilde{r} \\ 0 & \text{otherwise} \end{cases} . \quad (8)$$

Differentiating the above equation, we have

$$\vec{N}(x,y) = \left(\frac{\tilde{h}\cdot x}{\tilde{r}\sqrt{x^2+y^2}}, \frac{\tilde{h}\cdot y}{\tilde{r}\sqrt{x^2+y^2}}, 1 \right). \quad (9)$$

$$\vec{d}(x,y) = \left(\frac{\tilde{h}\cdot x}{\tilde{r}\sqrt{x^2+y^2}}, \frac{\tilde{h}\cdot y}{\tilde{r}\sqrt{x^2+y^2}} \right). \quad (10)$$

The conic model is a simple terrain model with equal steepness "almost everywhere" on the conic surface. A drawback is that it is not C^1 continuous at the apex and bottom rim.

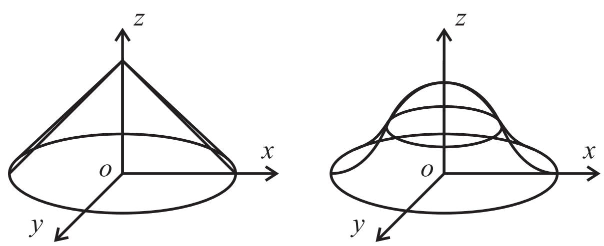

(a) Simple conic model (b) Smooth Gaussian model

Fig. 4. Terrain models.

2) Smooth Gaussian Model: Fig. 4(b) shows a Gaussian model, defined as:

$$z = \tilde{h}\cdot e^{-\frac{x^2+y^2}{2\tilde{r}^2}}, \quad (11)$$

where $\tilde{h}$ is the height of the terrain, and $\tilde{r}$ determines the width/steepness of the terrain. Differentiating the above equation yields:

$$\vec{N}(x,y) = \left(-\frac{x\cdot z}{\tilde{r}^2}, -\frac{y\cdot z}{\tilde{r}^2}, 1 \right), \quad (12)$$

$$\vec{d}(x,y) = \left(-\frac{x\cdot z}{\tilde{r}^2}, -\frac{y\cdot z}{\tilde{r}^2} \right). \quad (13)$$

We consider the Gaussian model appropriate for skiing slopes because it is C^1 continuous everywhere, and has smooth S-shaped fastest descent curves, which is suitable for skiing.

Other terrain models are possible, and are left as future work. For example, general terrains can be reasonably described with NURBS surfaces [17], whose differentials can be easily computed and whose shapes are defined by grids of control points. As another example, 3D terrain models could be constructed from topographic maps. These terrain modeling approaches are beyond the scope of the current paper, which focuses on modeling skier mobility.

IV. Mobility Model Details

This section provides the details of our skier mobility model. We begin with the group arrival model, and then present the group leader model, and the flocking model for group members.

A. Group arrival

Groups arrive at the apex of the terrain according to a Poisson process with a constant arrival rate $\tilde{\lambda}_G$. That is, the time interval δt between the arrivals of two groups is exponentially distributed and independent, obeying:

$$p(\delta t = x) = \tilde{\lambda}_G \cdot e^{-\tilde{\lambda}_G x}, x > 0. \quad (14)$$

The number of members G_i in the i-th group can be set to a fixed value, or generated randomly using a uniform distribution:

$$N_{G_i} \sim \mathrm{U}\left(1, \tilde{N}_{GM}\right), \quad (15)$$

where $\tilde{N}_{GM}$ denotes the maximum group size allowed.

B. Group Leader Movement

The invisible leader leads a group skiing downhill. To have full control of their speed and direction, skiers slide on the edges of the skis rather than the bottom surface of their skis. This naturally produces an S-shaped trajectory. According to the turning radius, there are slalom, giant slalom, super giant slalom trajectories, etc. We assume a large turning radius since the skiers are on a relatively unconstrained terrain.

We use a randomized sine function to produce the curvy trajectory swaying left and right along the fastest descent direction. The skier's acceleration mostly originates from the gravitational acceleration. We set an upper bound to the acceleration to be the gravitational acceleration modified by the inclination angle of advance. The velocity is the integral of acceleration over time and the displacement is the integral of velocity over time. Note that we employ physics terminology: velocity is a vector representing both direction and magnitude; speed is a scalar representing solely the magnitude of velocity.

1) Direction: At the start, the invisible leader of a skier group is deposited at the top of a mountain, where the terrain's gradient is either non-existent (for the conic model) or zero (for the Gaussian model). We set the initial azimuth angle θ to a uniformly distributed random number

$$\theta(0) \sim \mathrm{U}(0, 2\pi). \quad (16)$$

The periodical sine function $\sin(t)$ has a shape similar to the curvy trajectory of skiing. We use the sine function to dynamically adjust the azimuth angle θ according to Equation 17 to generate an S-shaped curve, as shown in Fig. 5.

$$\theta(t) = \tilde{\theta}\cdot \sin(s(t)), \quad (17)$$

where $\tilde{\theta}$ is a constant representing the maximum allowed value of θ, and $s(t)$ is the *phase* parameter of the sine function at time t. To randomize the rate at which the advance direction changes, we increase the sine function's phase parameter by different values in the equal time interval Δt, based on a random variable ξ that has a uniform distribution:

$$s(t+\Delta t) = s(t) + \Delta t \cdot \xi, \quad (18)$$

$$\xi \sim \mathrm{U}\left(\tilde{\xi}_0, \tilde{\xi}_1\right). \quad (19)$$

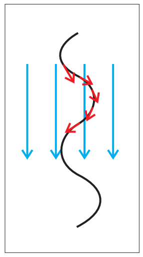

Fig. 5. Skiing directions (red) and terrain gradient (blue).

In the above equation, $\tilde{\xi}_0$ and $\tilde{\xi}_1$ are two constants specifying the lower and upper bounds of ξ.

2) Speed: Skiers gain speed from the gravitational force. The maximum acceleration of a skier is $\left|\vec{G}\right| \cdot \cos\varphi$, as determined by the gravitational acceleration $\left|\vec{G}\right|$ and the cosine value of the inclination angle of advance φ. Skiers decrease their speed by braking using their skis. The (negative) acceleration of braking depends on the skiing conditions (e.g., skis, wax, snow, temperature, humidity) and the skier's skill. To make the movement smooth, we suppose the skiers do not use all of their energy to brake, and the negative acceleration has a constant lower bound of $\tilde{A}_0$. The acceleration rate $\left|\vec{A}\right|$ is a random variable that has a uniform distribution:

$$\left|\vec{A}\right| \sim \mathrm{U}\left(\tilde{A}_0, \left|\vec{G}\right| \cdot \cos\varphi\right). \tag{20}$$

The speed is changed in a discrete fashion, with imposed constant lower and upper bounds $\tilde{V}_0$ and $\tilde{V}_1$, according to the following equation

$$\begin{aligned} &\left|\vec{V}(t+\Delta t)\right| \\ &= \max\left\{\tilde{V}_0, \min\left\{\tilde{V}_1, \left|\vec{V}(t)\right| + \left|\vec{A}(t)\right| \cdot \Delta t\right\}\right\}. \end{aligned} \tag{21}$$

In an infinitesimal time interval Δt, a skier advances in a direction determined by θ for a distance of

$$\Delta L = \left|\vec{V}(t)\right| \cdot \Delta t \tag{22}$$

on the terrain's surface. Because calculating the distance on an arbitrary surface is very difficult, we use a numerical method. To this end, we advance in the (x, y) parameter space gradually with very small time steps. In the kth step, the MN moves from the 3D point P_{k-1} to P_k on the terrain. After k steps, the cumulative distance travelled is:

$$L_k = \sum_{i=1}^{k} \left|P_{k-1}, P_k\right|. \tag{23}$$

The advance stops when $L_k \geq \Delta L$.

C. Flocking model

Because backcountry skiing is a risky sport, people usually do it in groups. Observing the behaviors of skiers in groups, we can find the following characteristics: (1) Group members ski along a similar path coherently, so that no group members drop out; (2) Each skier actively avoids collisions with other skiers, as well as obstacles and cliffs; (3) Skiers spontaneously coordinate their behaviors with their group members. We use a flocking model to simulate the movement of skiers in groups.

The *flocking model*, first proposed by Reynolds [16], is often grouped with *artificial life* algorithms because of its emergent behavior: complex global behaviors arise from the interaction of simple local rules. It has been successfully applied to artificial life, robotics, art, computer games, etc. In our flocking model, the three characteristics of group skiers are translated into three virtual forces, i.e., the cohesion force, the separation force, and the alignment force. The three forces keep a dynamical balance between skiers, and influence group members to follow the invisible leader, while keeping a safe distance from other skiers, and coordinating their movements within a group. Consequently, complex, life-like behaviors of skiers are achieved. We assume that each skier has the same weight, and thus, the composition of the forces is converted proportionally into *accelerations* of the skiers, which are limited by lower and upper bounds, calculated similarly to those for the invisible leaders. Then the skier's *velocity* is obtained by integrating the acceleration over time and the *displacement* is obtained by integrating the velocity over time.

1) Cohesion: The cohesion force pulls skiers in a group towards the invisible leader. As shown in Fig. 6(a), the cohesion force for the jth skier in the ith group, S_{ij}, with a 2D projected location p_{ij}, is defined as

$$\vec{F}_c(S_{ij}) = \tilde{c}_c \cdot (p_{ih} - p_{ij}), \tag{24}$$

where $\tilde{c}_c$ is the constant coefficient of the cohesion force, and p_{ih} is the 2D location of the invisible leader of group i. From the above equation we can see that the magnitude of the cohesion force depends linearly on the distance between p_{ij} and p_{ih}. That means when a skier is far from the invisible leader, the cohesion force will be dominant, and the skier will accelerate to rejoin the group.

2) Separation: The separation force steers skiers to avoid possible collisions. As shown in Fig. 6(b), for the skier colored in red, the separation forces come from all other skiers within a "visibility distance" $\tilde{d}_v$, regardless of the groups to which they belong. The separation force for the jth skier in the ith group, S_{ij}, at the 2D location p_{ij}, is defined as

$$\vec{F}_s(S_{ij}) = \tilde{c}_s \sum_{l=0}^{N_G-1} \sum_{k=0}^{N_{G_l}-1} \vec{F}_s(S_{ij}, S_{lk}), \tag{25}$$

where $\tilde{c}_s$ is a constant coefficient for the separation force, N_G is the number of groups, and N_{G_l} is the size of the lth group.

$$\vec{F}_s(S_{ij}, S_{lk}) = \begin{cases} 0, & \text{if } i = l \wedge j = k \\ & \vee \left|p_{lk} - p_{ij}\right| > \tilde{d}_v \\ \frac{p_{ij} - p_{lk}}{\left|p_{ij} - p_{lk}\right|^2}, & \text{otherwise} \end{cases}. \tag{26}$$

From the above equations, we can see that the magnitude of separation force between a pair of skiers within the visibility distance $\tilde{d}_v$ is inversely related to their distance. That means the closer two skiers are to each other, the stronger the separation force is. When two skiers are very close, the

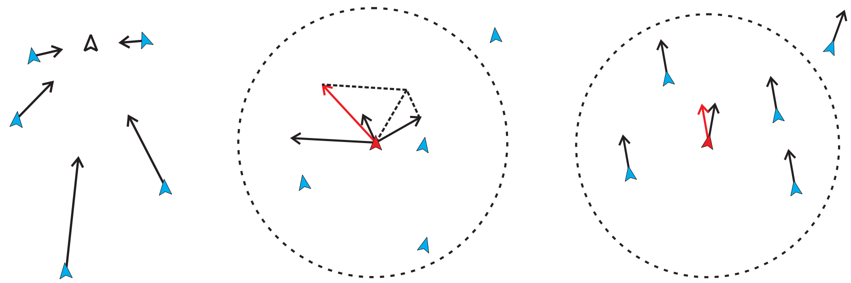

(a) Cohesion (b) Separation (c) Alignment

Fig. 6. Component forces of the flocking model.

separation force becomes dominant and steers them away from each other in order to avoid a possible collision.

3) Alignment: The alignment force adjusts the speeds and directions of a skier to be consistent with other group members. As shown in Fig. 6(c), a skier (colored in red) coordinates only with his/her team members within the "visibility distance" $\tilde{d}_v$. The alignment force for the jth skier in the ith group at the 2D location p_{ij} is calculated as

$$\vec{F}_a\left(S_{ij}\right) = \tilde{c}_a \frac{\sum_{k=0}^{N_{G_i}} \delta_{jk} \cdot \vec{v}_{ik}}{\sum_{k=0}^{N_{G_i}} \delta_{jk}}, \tag{27}$$

where $\tilde{c}_a$ is a constant coefficient of the alignment force, $\vec{v}_{ik}$ is the velocity of the kth skier in the ith group, and

$$\delta_{jk} = \begin{cases} 0, & \text{if } |p_{ij} - p_{ik}| > \tilde{d}_v \vee j = k \\ 1, & \text{otherwise} \end{cases}. \tag{28}$$

V. Simulation Experiments

In this section, we present some preliminary simulation results obtained using our skiing mobility model. We start with simulation validation experiments, and then present an example evaluating the rescue probabilities for backcountry skiers in the event of an avalanche. All simulation results presented in this section use the simple conic terrain model.

A. Model Validation

Our simulation model is implemented in Objective C ++ on Mac OS X. In addition to the mathematical model of skiing mobility in the simulator, we also built a visualization front-end for the simulator. The visualization component was used in initial testing, debugging, and validation of the mobility models. It is also useful in studying the sensitivity of skier movement to different mobility parameters (e.g., group size, speed, cohesion).

Fig. 7 shows examples of the visual validation[1] of our model. The diagrams depict an aerial view of the mountain, where the apex of the terrain is located at the center of the image. Fig. 7(a) shows the skiing tracks left by 20 different group leaders who have skied down the mountain. Fig. 7(b) shows the combined tracks produced by groups of skiers, each with 1 to 5 members. As evident from the diagrams, each group leader follows a well-defined descent direction, while swaying left and right along a sinusoidal curve. The trajectories of the group members are similar to those of the group leaders. The approximately parallel curves suggest that safe separation distances are maintained between skiers, and the group members are coordinated.

[1]We have also done further validation work to verify that the group arrival model is Poisson, and that velocity constraints are properly obeyed.

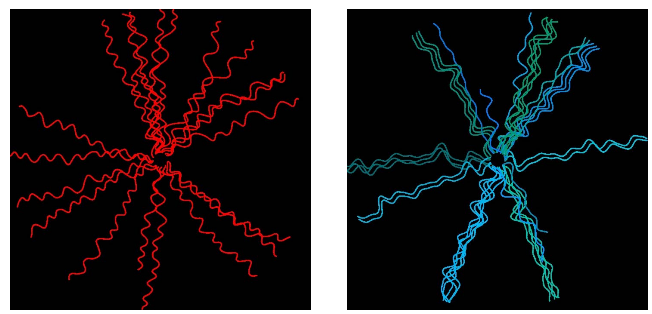

(a) Group leader trajectories (b) Group trajectories

Fig. 7. Visual validation of skier mobility model.

The resulting "tracks" in Fig. 7 are conceptually similar to the trajectories of real-world skiing. There are also sufficient elements of randomization within a group, to reflect the non-determinism of real-world skier mobility. We consider the resulting model suitable for our objectives.

B. Avalanche Scenarios

To demonstrate the usefulness of our model, we use it to study the avalanche rescue probability in a backcountry skiing scenario. In this scenario, groups of skiers are deposited on the top of a mountain via helicopter, and then ski down to the bottom of the mountain.

Backcountry skiing is a risky sport, with one of the primary threats being avalanches. Avalanches are unpredictable events that cause tons of snow to cascade down the side of a mountain, destroying everything in its path. Skiers are at great risk during avalanches, since they can be buried instantly under several meters of snow. Rescuers must find them within several minutes before they suffocate to death. Wireless communication devices, such as avalanche transponders, are the most important piece of safety equipment for backcountry skiers. Successful rescue is possible if a non-buried skier is within wireless range of a buried skier when the avalanche is over.

In our work, we evaluate the avalanche survival probability both with and without the wireless devices, using simulation. We also consider the effects of group size, wireless range, and skiing speed on the survival probability.

We use a very simple avalanche model in our initial study. Avalanches are modeled as random events that arrive according to a Poisson process. In our model, an avalanche covers a randomly chosen sector of the mountain. The avalanche sector is determined by its angular bisector ψ_a and angular width w_a, both of which are uniformly distributed random variables between 0 and 2π radians.

The default parameter settings for our simulation experiments are summarized in Table I. We assume that a skier within the avalanche sector gets buried with a probability of 60%, and that a buried skier is found and rescued if a non-buried skier is within wireless communication range ($\tilde{d}_c$) of the buried skier.

TABLE I
SIMULATION PARAMETER SETTINGS

Parameter	Notation	Value
Time Step	Δt	1/30 s
Group Arrival Rate	$\tilde{\lambda}_G$	8 s
Azimuth Angle	$\tilde{\theta}$	π/3
Lower Bound on Angle Deviation	$\tilde{\xi}_0$	0.1
Upper Bound on Angle Deviation	$\tilde{\xi}_1$	1
Lower Bound on Acceleration	$\tilde{A}_0$	- 4.905 m/s^2
Cohesion Force Coefficient	$\tilde{c}_c$	0.01
Separation Force Coefficient	$\tilde{c}_s$	20.0
Alignment Force Coefficient	$\tilde{c}_a$	0.125
Wireless Range	$\tilde{d}_c$	100 m

We study how the survival and rescue probabilities change with the group size, wireless range, and skiing speed, in three simulation experiments. For statistical purposes, we compute the average results from observing 100 simulated avalanche events. Simulation data is recorded regarding the number of skiers N_{skiers}, the number of buried skiers N_{buried}, and the number of rescued skiers N_{rescued}. The rescue rate is calculated as $N_{\text{rescued}}/N_{\text{buried}}$. The survival rate without wireless device is calculated as $(N_{\text{skiers}} - N_{\text{buried}})/N_{\text{skiers}}$. The survival rate with wireless device is calculated as $(N_{\text{skiers}} - N_{\text{buried}} + N_{\text{rescued}})/N_{\text{skiers}}$. The survival gain by using wireless devices is calculated as the difference between the foregoing two metrics.

In the first experiment, we fix the lower and upper bounds of speed to $\tilde{V}_0$ = 50 km/h and $\tilde{V}_1$ = 80 km/h and the size of each group to $1, 2, \cdots, 10$, respectively. The result is shown in Fig. 8. The width of avalanche sector has a uniform distribution between 0 and 2π, so it's mathematical expectation is π and the avalanche sector is expected to cover 50% of the terrain. The bury probability is 60%. Hence, we expect that the survival rate without wireless devices is 70%. The experimental result is consistent with this expectation.

As expected, the use of wireless devices improves survival rates for most group sizes. For single skiers (with group size 1), the wireless devices rarely help. The reason is that the skiers are scattered on the large mountain and the distances

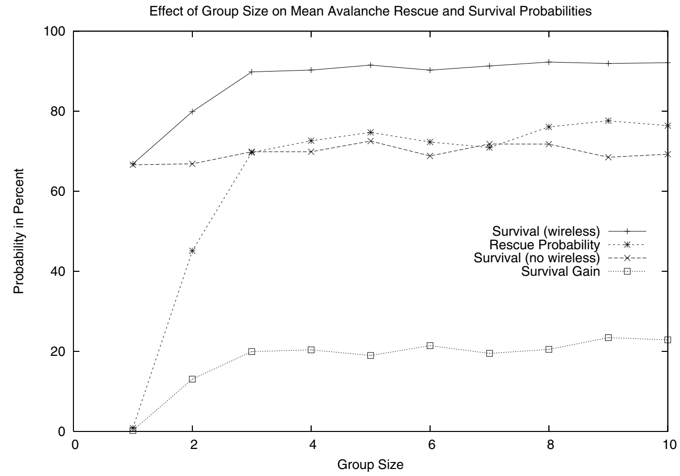

Fig. 8. Effect of group size on avalanche rescue and survival probability.

between them exceeds the wireless range. This also implies that rescues across groups are unlikely.

The wireless devices are mostly useful for within-group rescue operations. When each group has two members, the wireless devices improve survival rate by 13%. When each group has three members, the survival rate is further improved to 90%. When each group has more than three members, the average survival rate remains about the same, although the standard deviation (not shown here) continues to decrease. The rescue rates show similar trends as the gain of survival rate.

The results from this experiment suggest that: (1) wireless devices are helpful when skiing in groups; (2) a group composed of at least three persons should be formed when skiing; and (3) a larger group usually means a safer descent if wireless devices are used. These results all make sense intuitively.

In the second experiment, we fix the lower and upper bounds of speed to $\tilde{V}_0$ = 50 km/h, $\tilde{V}_1$ = 80 km/h, and the size of each group to 5, and the wireless range $\tilde{d}_c$ to 20, 30, ..., 180 m, respectively. The result is shown in Fig. 9. When $\tilde{d}_c \leq 40$ m, the survival probability is barely improved by using wireless devices, because skiers usually keep a distance greater than 40 m to avoid collision. The wireless devices show their values when $\tilde{d}_c \geq 50$ m, and the rescue probability is increased dramatically from 4% to 70% when $\tilde{d}_c$ increases from 60 to 90 m. The reason is that most skiers keep a minimum distance with other group members within this range. After a gradual increase when $\tilde{d}_c$ changes from 90 to 110 m, the rescue probability increases quickly again from 72% to 89%, when $\tilde{d}_c$ increases from 110 to 140 m. Within this range, a buried skier can have a better chance to reach two or more close skiers with the wireless devices. The survival probability with wireless devices reaches 96% when $\tilde{d}_c$ = 140 m. After that, the benefit gained by further increasing the wireless range is not obvious, because there are disastrous avalanches that bury all group members. This experiment suggests that the wireless devices used in backcountry skiing should have a communication range of at least 100 m, and 150 m highly preferred.

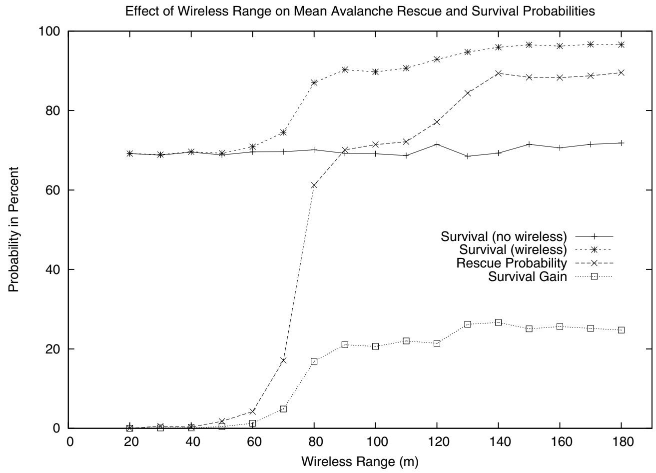

Fig. 9. Effect of wireless range on avalanche rescue and survival.

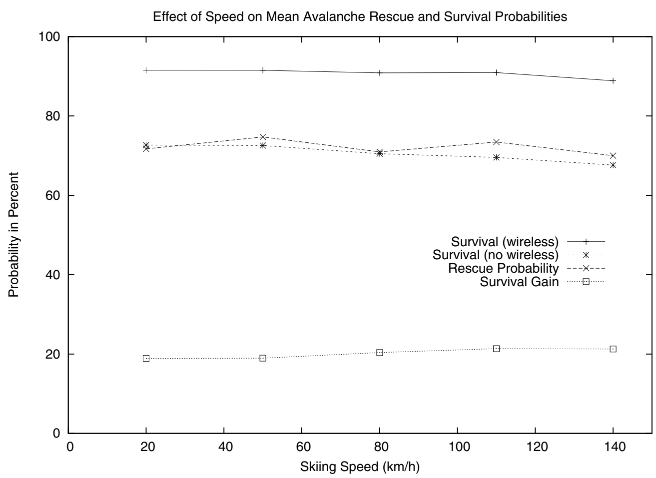

Fig. 10. Effect of skiing speed on avalanche rescue and survival.

We finally evaluate the survival and rescue rates at different skiing speeds. In this experiment, we fix the group size to 5, and vary the speed from low (20-50 km/h) to moderate (50-80 km/h), $\cdots$, up to Olympic racing speed (140-170 km/h). The results are shown in Fig. 10. From the results, we can see that as speed increases, the averages of survival and rescue rates decrease, the standard deviations increase (not shown), and the survival gain increases. The reason is that skiers are more likely to be further apart at higher speeds. However, all these changes are very slight. This experiment suggests that skiing speed has little impact on survival and rescue rates in the presence of avalanches, but increasing the speed does impair safety slightly, in which circumstance wireless devices help a bit more.

VI. Conclusion

In this paper, we presented a novel 2.5D skiing mobility model for mobile wireless ad hoc networks. This model is composed of groups of skiers. Each group has an invisible leader, who determines the overall direction and speed of the group's movement. We use a randomized sine function to produce a curvy trajectory and the gravitational acceleration modified by the inclination angle of advance to compute the maximum acceleration for the invisible leader. The movement of skiers in a group is determined by a flocking model, which translates the cohesion, separation, and alignment constraints into three virtual forces. The flocking model showed realistic life-like motions of skiers.

We used the proposed skiing mobility model to evaluate the survival and rescue probabilities of backcountry skiing in the presence of avalanches. We believe, however, that the proposed skiing mobility model can find additional uses in group mobility applications in wireless ad hoc networks.

Acknowledgment

The authors thank the anonymous reviewers for their helpful comments on our paper. Financial support for this research was provided by iCORE (Informatics Circle of Research Excellence) in the Province of Alberta, as well as NSERC (Natural Sciences and Engineering Research Council) in Canada.

References

[1] T. Camp, J. Boleng, and V. Davies, "A survey of mobility models for ad hoc network research," *Wireless Communications and Mobile Computing*, vol. 2, no. 5, pp. 483–502, 2002.

[2] F. Bai and A. Helmy, "A survey of mobility models in wireless adhoc networks," *Wireless Ad Hoc and Sensor Networks, Kluwer Academic Publishers*, 2004.

[3] M. Zonoozi and P. Dassanayake, "User mobility modeling and characterization of mobility pattern," *IEEE Journal on Selected Areas in Communications*, vol. 15, no. 7, pp. 1239–1252, 1997.

[4] V. Davies, "Evaluating mobility models within an ad hoc network," Ph.D. dissertation, Colorado School of Mines, 2000.

[5] Z. Haas, "A new routing protocol for reconfigurable wireless networks," in *the IEEE International Conference on Universal Personal Communications (ICUPC)*, 1997, pp. 562–565.

[6] P. Johansson, T. Larsson, N. Hedman, B. Mielczarek, and M. Degermark, "Scenario-based performance analysis of routing protocols for mobile ad-hoc networks," in *International Conference on Mobile Computing and Networking (MobiCom)*, 1999, pp. 195–206.

[7] G.-L.-A. J.J and M. Spohn, "Source-tree routing in wireless networks," in *the 7th International Conference on Network Protocols (ICNP)*, 1999.

[8] W. Hsu, K. Merchant, H. Shu, C. Hsu, and A. Helmy, "Weighted waypoint mobility model and its impact on ad hoc networks," *ACM SIGMOBILE Mobile Computing and Communications Review*, vol. 9, no. 1, p. 63, 2005.

[9] V. Tolety, "Load reduction in ad hoc networks using mobile servers," Ph.D. dissertation, Colorado School of Mines, 1999.

[10] J. M.Ng and Y. Zhang, "A mobility model with group partitioning for wireless ad hoc networks," in *the Third International Conference on Information Technology and Applications*, 2005.

[11] F. Wang, B. Huang, and K. Ibrahim, "A survey of group merge and split mobility models," *UbiCC Journal*, vol. 2, no. 5, pp. 1–10, 2007.

[12] X. Hong, M. Gerla, G. Pei, and C. Chiang, "A group mobility model for ad hoc wireless networks," in *ACM International Workshop on Modeling and Simulation of Wireless and Mobile Systems*, 1999.

[13] M. Bergamo, "System design specification for mobile multimedia wireless network," Tech. Rep. DARPA project DAAB07-95-C-D156, 1996.

[14] J. Haerri, F. Filali, and C. Bonnet, "Mobility models for vehicular ad hoc networks: a survey and taxonomy," *EEE Communications Surveys and Tutorials*, 2008.

[15] F. Bai, N. Sadagopan, and A. Helmy, "The important framework for analyzing the impact of mobility on performance of routing protocols for adhoc networks," *Ad Hoc Networks*, vol. 1, no. 4, pp. 383–403, 2003.

[16] C. W. Reynolds, "Flocks, herds and schools: A distributed behavioral model," in *The 14th Annual Conference on Computer Graphics and Interactive Techniques (SIGGraph)*. ACM, 1987, pp. 25–34.

[17] L. A. Piegl and W. Tiller, *The NURBS book*. Springer Verlag, 1997.